Exploration of NavIC/GPS Receiver in both Static and Dynamic Way in an Open Surface/Ground Area

Mohmad Umair Bagali[1], Dr. Thangadurai N[2]*

[1]*Research Scholar, Department of Electronics and Communication Engineering,*

[2]*Professor and Research Coordinator, Department of Electronics and Communication Engineering, Faculty of Engineering Technology, CET, JAIN (Deemed-to-be University), Bengaluru, India.*

Abstract: Indian Regional Navigation Satellite System (IRNSS)/NavIC operates in two frequency bands namely L5 band (1176.45 MHz) and S1 band (2492.02 MHz). To navigate over vegetated area or man-made structures or unstructured area, different methods have been used. By utilizing NavIC user receiver along with comparison with GPS leads to accurate navigation and near real time observation for this scenario. Various field surveys have been conducted by keeping one receiver as base station i.e., NavIC receiver kept constant and other receiver used as rover receivers. These base stations depend on the exact coordinates. In this study two fixed NavIC receivers and a rover receiver are used. By solving the distances between fixed points, and also by using the inverse distance weighting method, the error of rover receiver is found. It can be implemented anywhere, therefore local navigation system can be achieved easily.

Keywords: Carrier to Noise Ratio, Ionodelay, CEP, Positional Error

1. Introduction

Navigation is one of the key parameters in our each day lives. The vital navigational skills are employed to human beings such as going to work region or taking walks to school and so on. Navigation aids are greater complicated because the involvement of electronic transmission of the indicators and these are termed as radio-navigation aids. The Indian Regional Navigation Satellite System (IRNSS), is an indigenous, autonomous, regional navigation device is being bolstered via the Indian Space Research Organization. The IRNSS is being developed in parallel to the GPS Aided GEO Augmented Satellite Navigation (GAGAN) program; consequently the Satellite Based Augmentation System (SBAS) covers the corrections of GNSS signal. The IRNSS constellation consists of satellite named as 1A, 1B, 1C, 1D, 1E, 1F,1G, 1H and 1I. 1I is launched because of the failure of the satellite 1A as the Rubidium atomic clock was once not functioning. IRNSS consists of three geostationary satellites or Geosynchronous Equatorial Orbit (GEO) satellites and four Inclined Geo Synchronous Orbit (IGSO) satellites in contrast to the GPS constellation, which consists of only Medium Earth Orbit (MEO) satellites (Fig.1) These troubles related with GEO satellites are now not restricted to IRNSS as they can be observed in BeiDou and Satellite-Based Augmentation System (SBAS) GEO satellites that grant ranging information. One such section of SBAS is the Wide Area Augmentation System (WAAS), which transmits ranging information. Differential IRNSS is a technique that wishes to have one or numerous base stations on acknowledged positions and a rover receiver. The base stations grant correction for rover receiver.

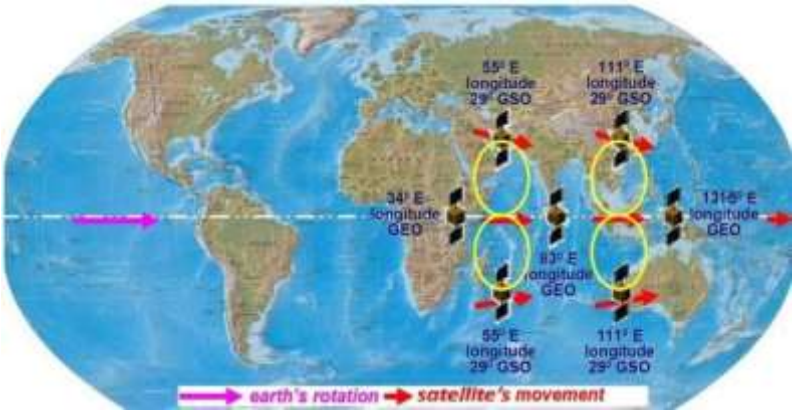

Fig. 1 NavIC/ **IRNSS Constellation**

DOP completely determines the geometry of the satellites. The relation of rms positional error to rms of pseudorange error is as follows

$$\sigma_{\text{Positional error}} = \text{DOP} * \sigma_{\text{pseudorange}} \quad \ldots\ldots\ldots\ldots$$

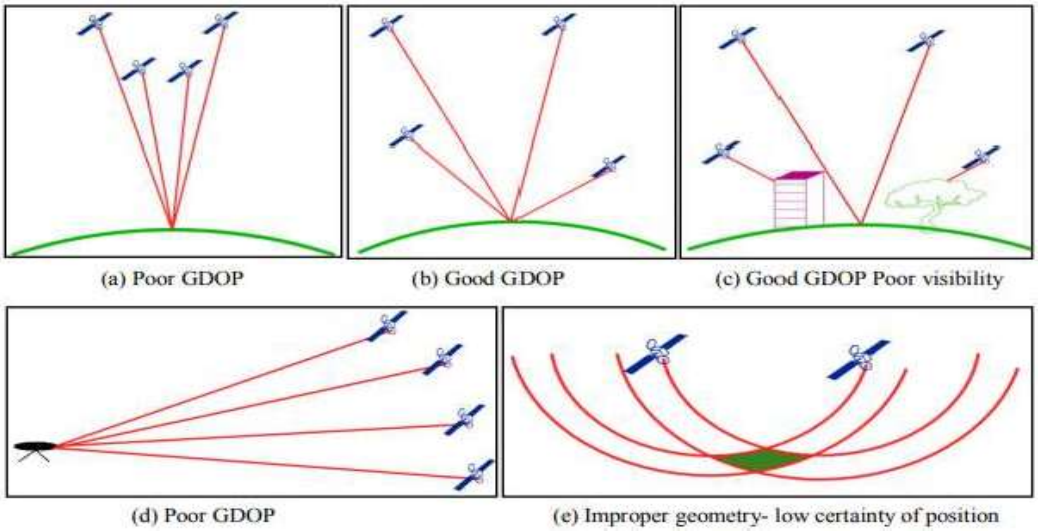

Fig. 2 GDOP visibility geometry

Whenever the satellite geometry is such that all the satellites are close together or not spread uniformly in the sky, the overlap between them is much larger, increasing more uncertainty of the GPS location to be than the condition when visible satellites are spread properly are far apart. The Figure 2 (e) demonstrated how the satellite geometry decides the uncertainty in the position.

2. Literature Review

For a static user in a multipath environment, the multipath error of GEO satellite in the code and provider section measurements will exchange progressively over quite a few hours due to the fact relative motion between the user and the satellite is minimal (Landau et al. 2013; Wang et al. 2015). In satellite navigation, the distance measured between the user and a satellite is called pseudorange (Parkinson et al. 1996a). The time period "range" is prefixed with "pseudo" due to the fact statement consists of person clock bias. A receiver measures pseudorange given as

$$\rho_r^{iSf} = R_r^{iSf} + dR^{iS} + c(dt_r - dT^{iS}) + I^{iSf} + T^{iS} + \mu\rho_r^{iSf} + B_r^{iSf} + \varepsilon\rho_r^{iSf} \quad \ldots (2)$$

where □ is the pseudorange (m), „r" indicates the receiver under test, „i" is the

observed satellite, „f" is the symbol for carrier frequency in the GNSS satellite system „S", R is the true geometric range (m), dR is the satellite orbital error (m), dt and dT are the receiver and satellite clock errors respectively (s), c is the speed of light (m/s), I is the ionospheric error (m), T is the tropospheric error (m), □□ is the code multipath error (m), B is the sum of inter- channel hardware bias, inter-frequency bias, and cross-correlation errors (m), and □□ is the receiver code noise (m).

Differencing code observations from a reference station to the user receiver minimizes atmospheric errors along with satellites orbital error and satellite tv for pc clock error. The reference station and person receiver are additionally called "base" and "rover" respectively. The distance between base and rover is named "baseline" and normally varies from a few metres to heaps of kilometers. This method is called Differential GPS (DGPS), and marine navigation makes use of it widely. The differencing between base and rover observations can be modelled as

$$\Delta\rho_{b,r}^{iSf} = \Delta R_{b,r}^{iSf} + \Delta dR^{iS} + c(\Delta dt_{b,r}) + \Delta I^{iSf} + \Delta T^{iS} + \Delta\mu\rho_{b,r}^{iSf} + \Delta B_{b,r}^{iSf} + \Delta\varepsilon\rho_{b,r}^{iSf} \quad \ldots (3)$$

where Δ stands for the differencing observations between base „b" and rover „r" receivers.

3. Methodology

The Time Difference Of Arrival (TDOA) of a signal can be estimated by two methods: 1) By subtracting TOA measurements from two base stations to produce a relative TDOA, 2) Through the use of cross-correlation techniques, in which the received signal at one base station is correlated with the received signal at another base station.

For a signal, s(t), radiating from a remote source through a channel with interference and noise, the general model for the time-delay estimation between received signals at two base stations, $x_1(t)$ and $x_2(t)$, is given by equation (4 and 5):

$$x_1 = A_1 s\ t - d_1\ + n_1(t) \quad \ldots(4)$$

$$x_2 = A_2 s\ t - d_2\ + n_2(t) \quad \ldots(5)$$

where A_1 and A_2 are the amplitude scaling of the signal, $n_1(t)$ and $n_2(t)$ consist of noise and interfering signals and d_1 and d_2 are the signal delay times, or arrival times.

If any or all of the receiver noise, multipath, receiver cross-correlation error and inter- channel bias are of large magnitude, mitigation methods are required before performing using the base and rover observations. Between-receiver differencing and between-satellite differencing can be completed in any sequence. Each receiver receives some strings which have different data, such as: longitude, latitude, altitude, etc. Another important data received from satellite is Dilution of Precision (DOP). By putting two IRNSSS receivers on two points, the distance between them can be calculated.

The Great Circle Calculation is the shortest distance between two points on the surface of the Earth which is calculated in two ways

a) Haversine Formula

$$d = 2 \times R \times \arcsin\left(\sqrt{\sin^2\left(\frac{\varphi_2 - \varphi_1}{2}\right) + \cos(\varphi_1)\cos(\varphi_2)\sin^2\left(\frac{\lambda_2 - \lambda_1}{2}\right)}\right) \quad \ldots(6)$$

b) Spherical Law of Cosines

$$d = \arccos\left(\sin(\varphi_1)\times\sin(\varphi_2)+\cos(\varphi_1)\times\cos(\varphi_2)\times\cos(\Delta\lambda)\right)\times R \quad \ldots (7)$$

Where R is the radius of the earth in specified latitude, a – an equatorial radius, b – a polar radius, e – the eccentricity of the ellipsoid, distance between the two points – d, λ longitudes points and φ are latitude points.

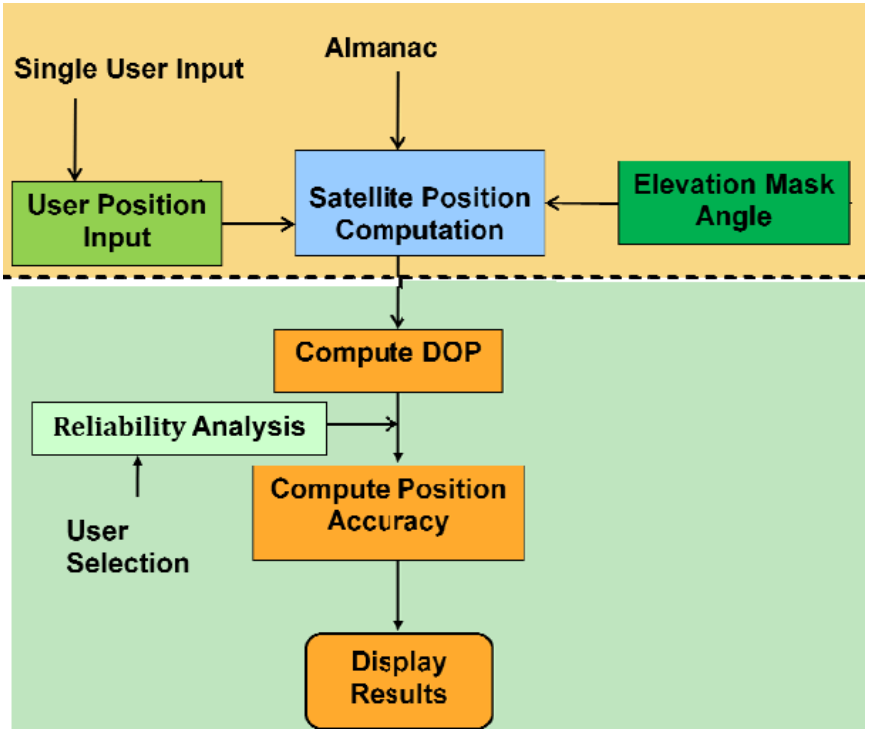

4. Field Surveys

The TLE is a data format encoding a list of orbital elements of an Earth-orbiting object for a given particular point of time and TLE File – 1 represents for GPS and File – 2 for IRNSS.

TLE File - 1
1 39199U 13034A 18286.08312216 .00000101 00000-0 00000+0 0 9991
2 39199 29.6556 106.8106 0020462 175.0043 185.0772 1.00267130 19530

TLE File – 2
1 41469U 16027A 18286.28058308 -.00000353 00000-0 00000-0 0 9991
2 41469 3.2448 252.5767 0004151 222.6039 137.1292 1.00277421 9082

NavIC receivers are used to gather and save data are needed to store. To do that, a hardware which is shown in Fig. 3 (a) and (b) is designed and connected to the receiver. In this hardware, IRNSS/ NavIC/GPS user receiver is used to receive signals from satellites. To save receiving data, raspberry pi is used and to work for long hours, an external battery is used. Fig. 4 shows the antenna mounted on rover for field survey tests.

(a) (b)

Fig. 3 (a) Front view and (b) Back view of the Hardware setup for field survey

Fig. 4 Antenna mounted on rover

5. Results and Discussion

On 12th October 2018, Thursday there was a survey conducted in Cricket ground of Jain Global Campus. The two receivers were taken for the survey. The two receiver kept apart 30 meters away facing North to South. Out of these two receivers one was static and one was dynamic. The dynamic receiver for every one meter it was moved and the reading were taken accordingly. The same procedure has been repeated from East to West. The data was also collected from the laptop. Throughout the survey we were able to observe variations in all 6 satellites which were represented in a graph. The skyplot at the end of the survey was observed. The latitude, longitude, altitude, TOWC, Doppler effect, carrier delay, tropospheric delay and the ionosphere delay was observed throughout the survey and the graphs was plotted.

Case (i)
Receiver A37 is in Dynamic state

Table 1: DOP when A37 in Dynamic state

TOWC (s)	GDOP	PDOP	HDOP	VDOP	TDOP	Total No of Satellites	Total No of IRNSS Satellites	Total No of GPS Satellites	Position Mode
456005	2.04711	1.69629	0.87789	1.45144	1.14597	14	7	7	7
456006	2.04725	1.69640	0.87788	1.45158	1.14606	14	7	7	7
456007	2.04739	1.69651	0.87787	1.45172	1.14615	14	7	7	7
456008	2.04753	1.69662	0.87786	1.45186	1.14623	14	7	7	7
456009	2.04767	1.69673	0.87785	1.45199	1.14632	14	7	7	7
456010	2.04781	1.69685	0.87784	1.45213	1.14640	14	7	7	7
456011	2.04795	1.69696	0.87782	1.45227	1.14649	14	7	7	7
456012	2.04809	1.69707	0.87781	1.45241	1.14657	14	7	7	7
456013	2.04823	1.69718	0.87780	1.45254	1.14666	14	7	7	7

Table 2: DOP when A38 in Static state

TOWC (s)	GDOP	PDOP	HDOP	VDOP	TDOP	Total No of Satellites	Total No of IR Satellites	Total No of GP Satellites	Position Mode
456005	1.7478	1.4457	0.7365	1.2440	0.9823	16	7	9	7
456006	1.7479	1.4457	0.7365	1.2440	0.9823	16	7	9	7
456007	1.7479	1.4457	0.7365	1.2441	0.9823	16	7	9	7
456008	1.7479	1.4457	0.7365	1.2441	0.9824	16	7	9	7
456009	1.7479	1.4458	0.7364	1.2442	0.9824	16	7	9	7
456010	1.7480	1.4458	0.7364	1.2442	0.9824	16	7	9	7
456011	1.7480	1.4458	0.7364	1.2442	0.9824	16	7	9	7
456012	1.7480	1.4458	0.7363	1.2443	0.9824	16	7	9	7
456013	1.7481	1.4459	0.7363	1.2443	0.9824	16	7	9	7

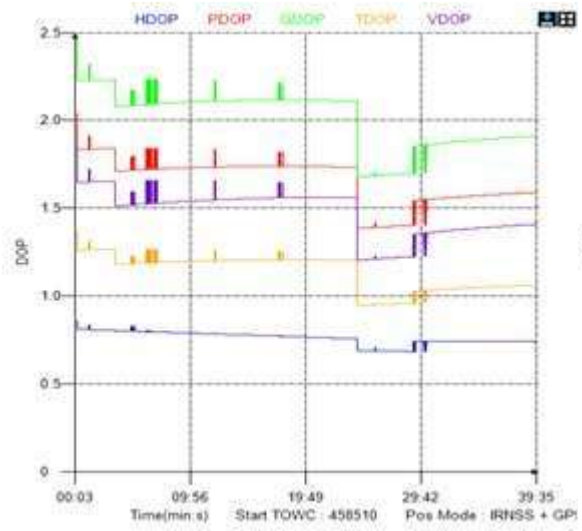

Fig.5 (a) A38 in Static mode

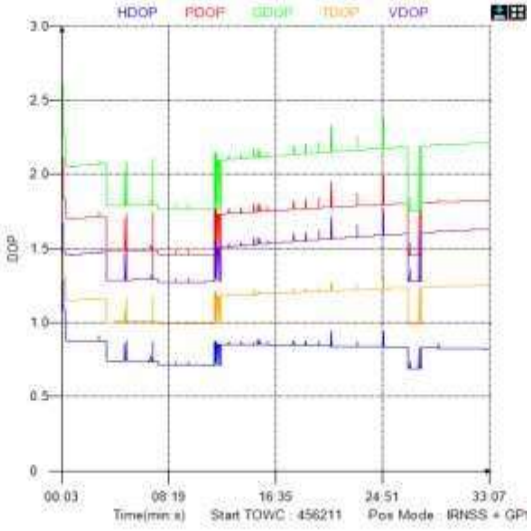

Fig.5 (b) A37 in Dynamic mode

Fig .5(c) A37 Dynamic and A38 Static Static

Fig .5(d) A38 Dynamic and A37

Fig .5(e) A37 receiver Antenna in static dynamic

Fig .5(f) A38 receiver antenna in

Figure 5 (a) and (b) shows the dilution of precision of the collected data when A37 is dynamic mode and A38 in static mode. There is a relation between the DOP and number of satellite visibility. As the visibility of satellite come down the DOP increase that can be observed in the plots (Table 1 and 2). Figure 5(e) shows the antenna of A38 dynamic receive mode kept on the cricket ground and plotting rover receiver with real time data plot shown in figure 5(c) i.e., red points shows the dynamic movement of A37 receiver and blue points represents the A38 static observation. Similarly figure 5(d) red points shows the static observation from A37 receiver and blue points represents the A38 dynamic movement observation in corresponding plotted in Google map. Fig. 5(e) shows the A37 receiver antenna mount on ground which is in static position whereas the A38 receiver antenna mounted on top of vehicle act as the dynamic state when it is moving towards to the receiver A37.

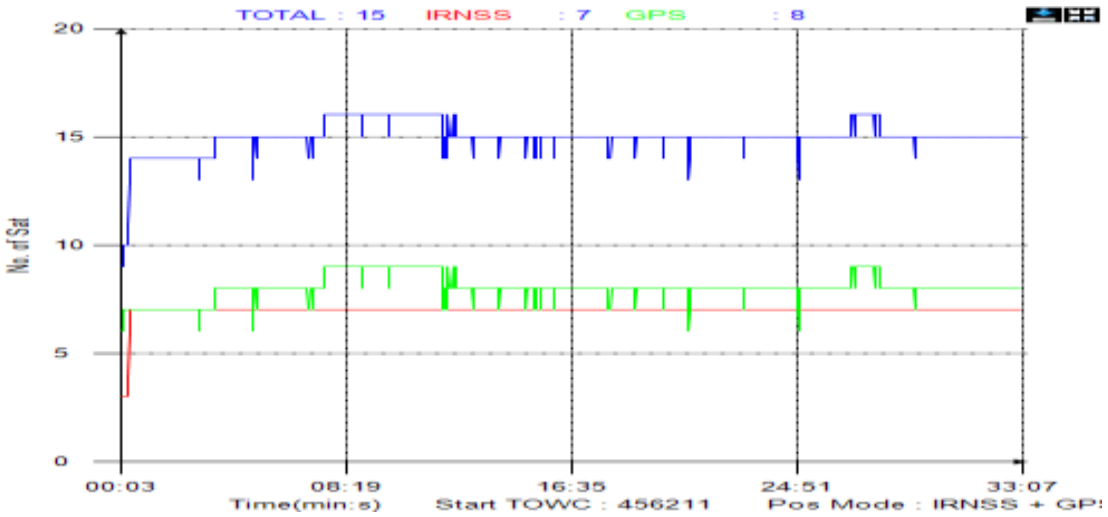

Fig.6 Number of satellites v/s TOWC in all 3 modes

Table 3 Positional values in case (i)

A37 Dynamic			A38 Static		
Latitude (deg)	Longitude (deg)	Altitude (m)	Latitude (deg)	Longitude (deg)	Altitude (m)
12.63851	77.44122	616.031	12.6384	77.4415	616.7759
12.63851	77.44122	616.0528	12.6384	77.4415	616.4939
12.63851	77.44122	615.375	12.6384	77.4415	616.3983
12.63851	77.44122	615.0501	12.6384	77.4415	616.6962
12.63852	77.44122	615.0161	12.6384	77.4415	616.4915
12.63851	77.44122	615.3763	12.6384	77.4415	616.6776
12.63851	77.44122	615.5405	12.6384	77.4415	616.4500
12.63851	77.44122	615.3326	12.6384	77.4415	616.5851
12.63851	77.44122	616.337	12.6384	77.4415	616.4234
12.63851	77.44122	615.9829	12.6384	77.4414	616.4859

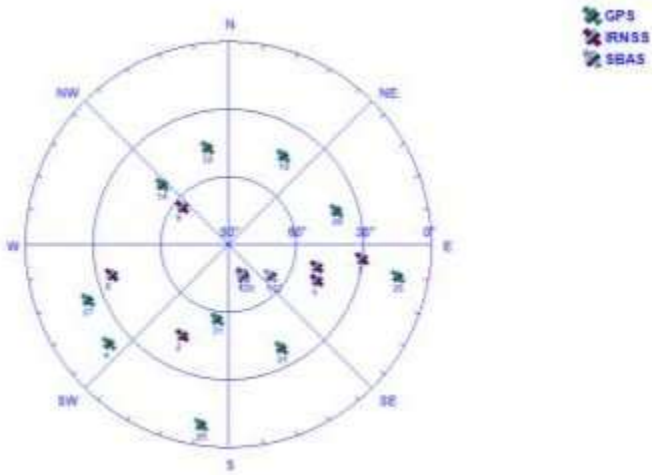

Fig.7 Sky plot of all the satellites for the entire survey duration

Figure 6 gives the overall view of the satellite visibility during the survey i.e., 33 minutes including both IRNSS and GPS satellites and SBAS satellite used for corrections

shown in sky plot in Fig. 7. From Table 3 it can be observed that the minor variation in the positional values i.e., latitude, longitude and altitude when receiver A37 kept as dynamic and A38 receiver is in static condition and moving towards the receiver A37.

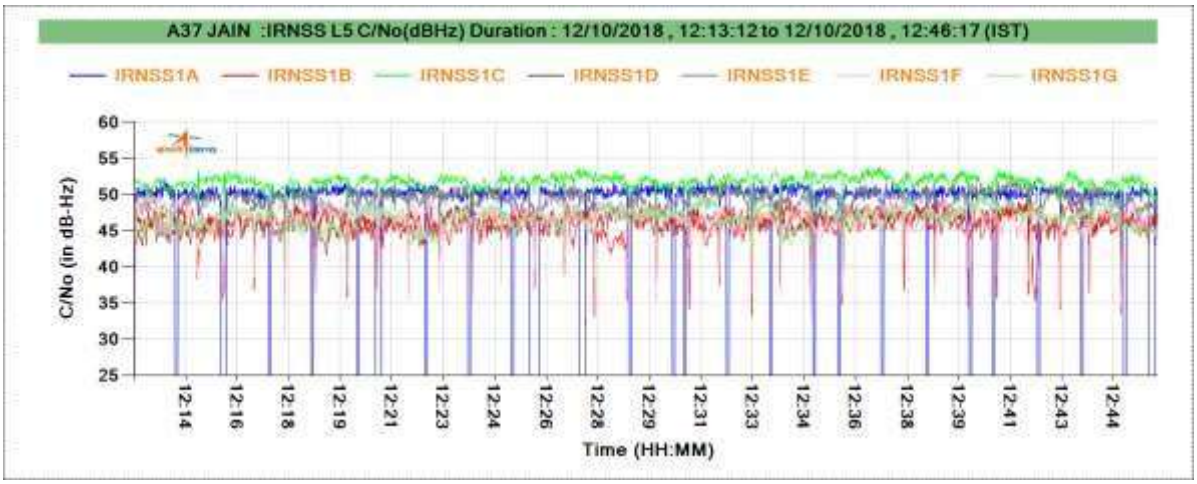

Fig .8(a) IRNSS L5 Band C/N_0

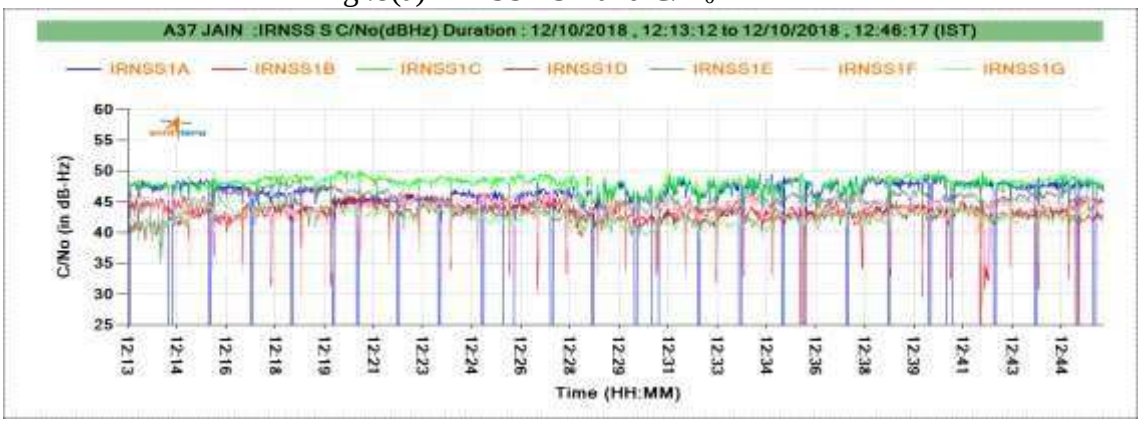

Fig .8(b) IRNSS S1 Band C/N_0

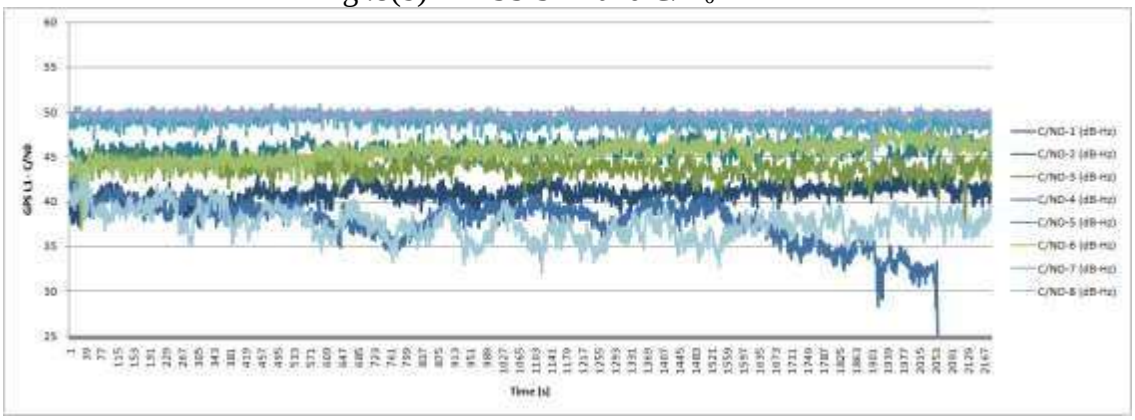

Fig .8(c) GPS L1 Band C/N_0

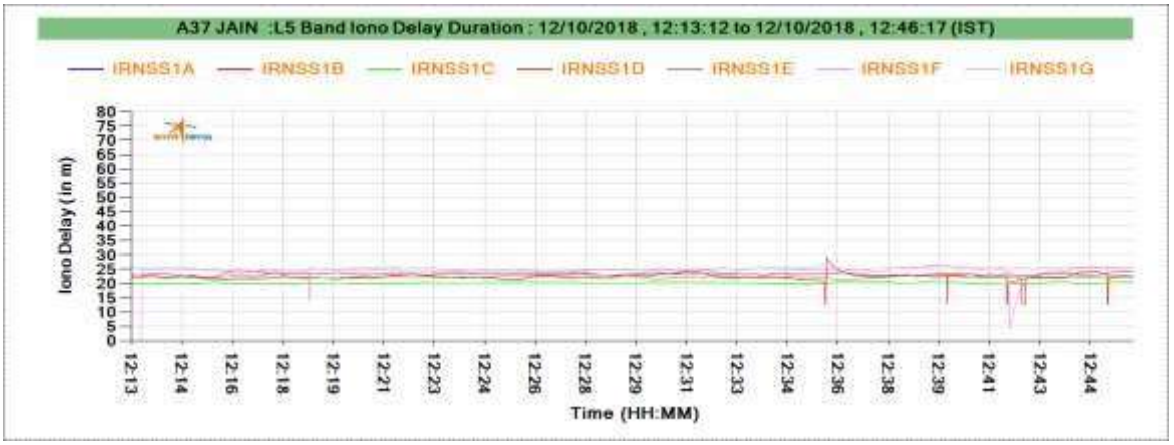

Fig .8(d) IRNSS L5 Band Iono delay

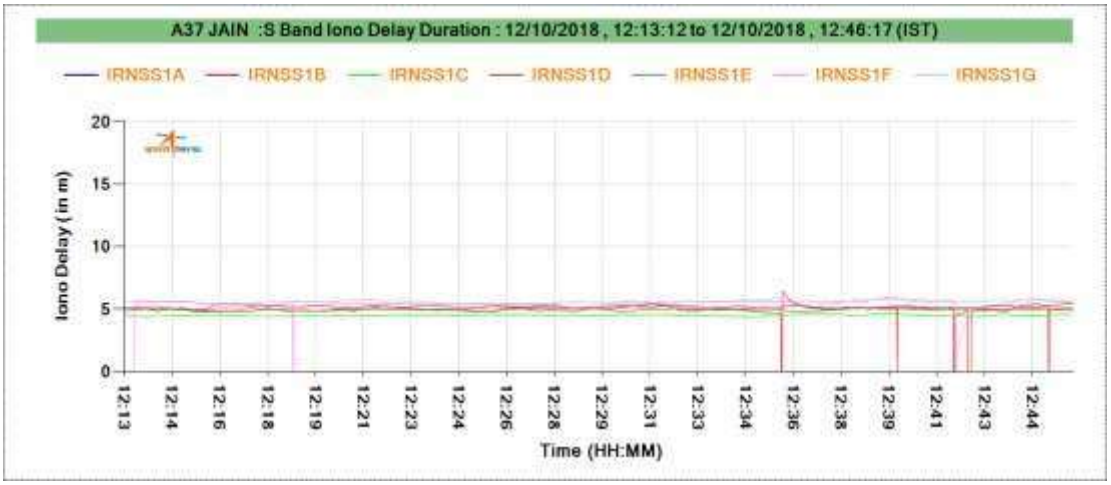

Fig .8(e) IRNSS S1 Band Iono delay

IRNSS 1A to IG and GPS L1 C/N0 and Iono delay observation plots shown in Fig. 8(a) to (e) based on the A37 in dynamic and A38 in static mode during the whole testing survey period. IRNSS C/N_0 varies from 46.37 to 51.9 whereas in case of GPS varies from

to 51. Fig. 9 shows the variations in the CEP error when A38 is moving towards the A37 receiver.

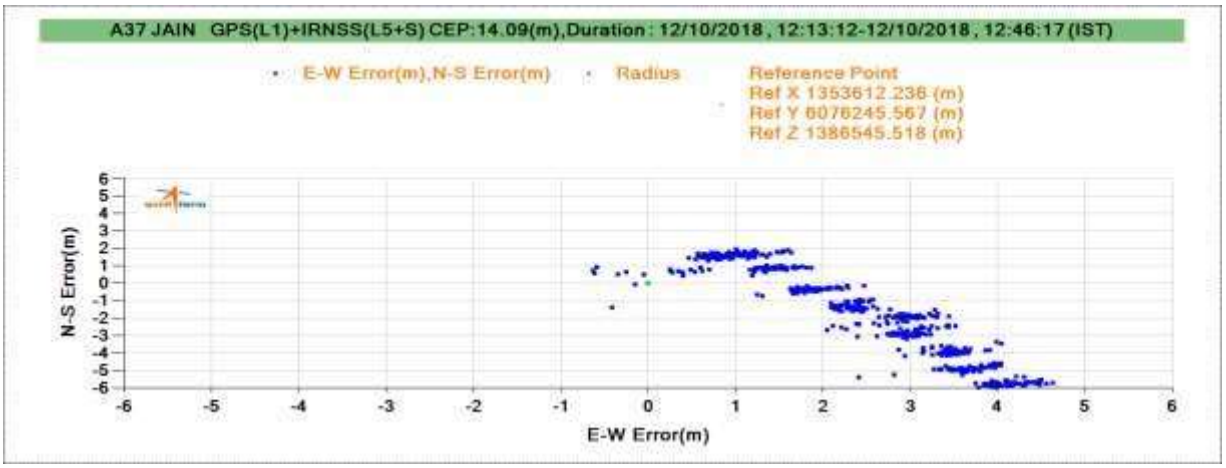

Fig.9 CEP error plot during survey

Case (ii)

Receiver A37 is in Static state

Table 4 DOP when A37 is in Static state

TOWC (s)	GDOP	PDOP	HDOP	VDOP	TDOP	Total No of Satellites	Total No of IRNSS Satellites	Total No of GPS Satellites	Position Mode
458846	1.8145	1.4946	0.83323	1.240905	1.028846	15	6	9	7
458847	1.8146	1.4947	0.833247	1.240969	1.028896	15	6	9	7
458848	1.8147	1.4948	0.833264	1.241033	1.028945	15	6	9	7
458849	1.8148	1.4948	0.833281	1.241097	1.028995	15	6	9	7
458850	1.8148	1.4949	0.833298	1.241161	1.029044	15	6	9	7
458851	1.8149	1.495	0.833315	1.241225	1.029094	15	6	9	7
458852	1.8150	1.495	0.833332	1.241289	1.029143	15	6	9	7
458853	1.8151	1.495	0.833349	1.241353	1.029193	15	6	9	7
458854	1.8152	1.4951	0.833366	1.241417	1.029242	15	6	9	7

Table 5 DOP when A38 is in Dynamic state

TOWC (s)	GDOP	PDOP	HDOP	VDOP	TDOP	Total No of Satellites	Total No of IRNSS Satellites	Total No of GP Satellites	Position Mode
458846	2.0875	1.7175	0.7971	1.5213	1.1865	16	7	9	7
458847	2.0875	1.7175	0.7971	1.5213	1.1866	16	7	9	7
458848	2.0876	1.7176	0.7971	1.5214	1.1866	16	7	9	7
458849	2.0877	1.7176	0.7970	1.5215	1.1866	16	7	9	7
458850	2.0877	1.7177	0.7970	1.5216	1.1867	16	7	9	7
458851	2.0878	1.7177	0.7970	1.5217	1.1867	16	7	9	7
458852	2.0879	1.7178	0.7969	1.5217	1.1868	16	7	9	7
458853	2.0880	1.7178	0.7969	1.5218	1.1868	16	7	9	7
458854	2.0880	1.7179	0.7969	1.5219	1.1869	16	7	9	7

Fig.10 (a) A37 in Static mode Fig.10 (b) A38 in Dynamic mode

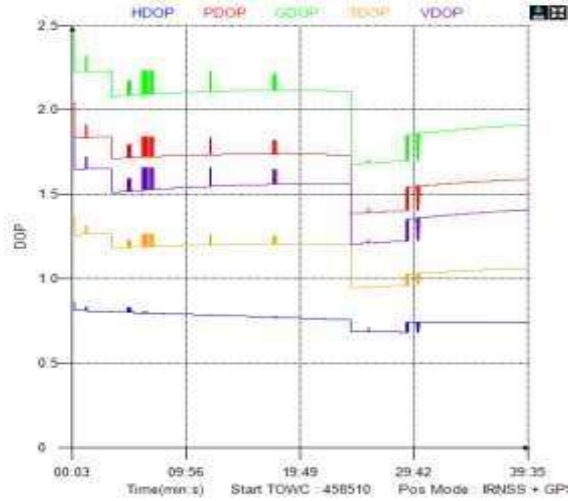

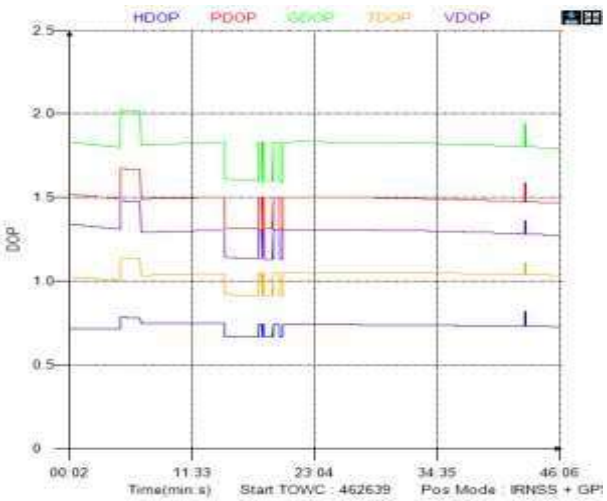

Fig .10(c) A37 Dynamic and A38 Static Static

Fig .10(d) A38 Dynamic and A37

Fig .10(e) A38 receiver antenna in Static dynamic

Fig .10(f) A37 receiver antenna in

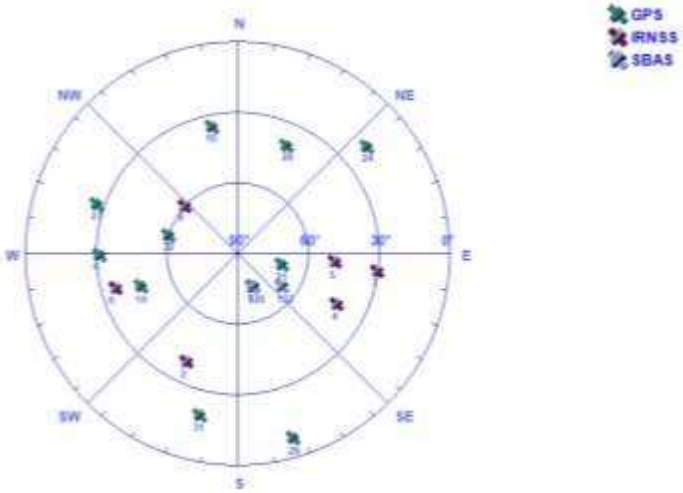

Fig.11 Sky plot of all the satellites for the entire survey duration

Figure 10 (a) and (b) shows the dilution of precision of the collected data when A38 is dynamic mode and A37 in static mode. There is a relation between the

DOP and number of satellite visibility. As the visibility of satellite come down the DOP increase that can be observed in the plots (Table 3 and 4). Figure 10(e) shows the antenna of A37 dynamic receive mode kept on the cricket ground and plotting rover receiver with real time data plot shown in figure 10(c) i.e., yellow + green points shows the dynamic movement of A37 receiver and blue points represents the A38 static observation. Similarly figure 10(d) green points shows the static observation from A37 receiver and red points represents the A38 dynamic movement observation in corresponding plotted in Google map (Fig, 10.(e) and (f)).

Table 6 Positional values in case (ii)

A37 Static			A38 Dynamic		
Latitude (deg)	Longitude (deg)	Altitude (m)	Latitude (deg)	Longitude (deg)	Altitude (m)
12.63858	77.44138	611.22340	12.63841	77.44147	615.3423
12.63858	77.44138	611.84490	12.63841	77.44147	615.4733
12.63858	77.44138	612.04900	12.63841	77.44147	615.3175
12.63858	77.44138	612.12160	12.63841	77.44147	615.3559
12.63858	77.44138	611.80790	12.63841	77.44147	615.2071
12.63858	77.44138	611.89890	12.63841	77.44147	615.6131
12.63858	77.44138	611.89790	12.63841	77.44147	615.3948
12.63858	77.44138	612.06880	12.63841	77.44147	615.2695
12.63858	77.44138	611.57880	12.63841	77.44147	615.0041
12.63858	77.44138	611.58790	12.63841	77.44147	615.2807

The overall view of the satellite visibility during the survey i.e., 33 minutes including both IRNSS and GPS satellites and SBAS satellite used for corrections shown in sky plot in Fig. 11. From Table 6 it can be observed that the minor variation in the positional values i.e., latitude, longitude and altitude when receiver A37 kept as static and A38 receiver is in dynamic condition and moving towards the receiver A37.

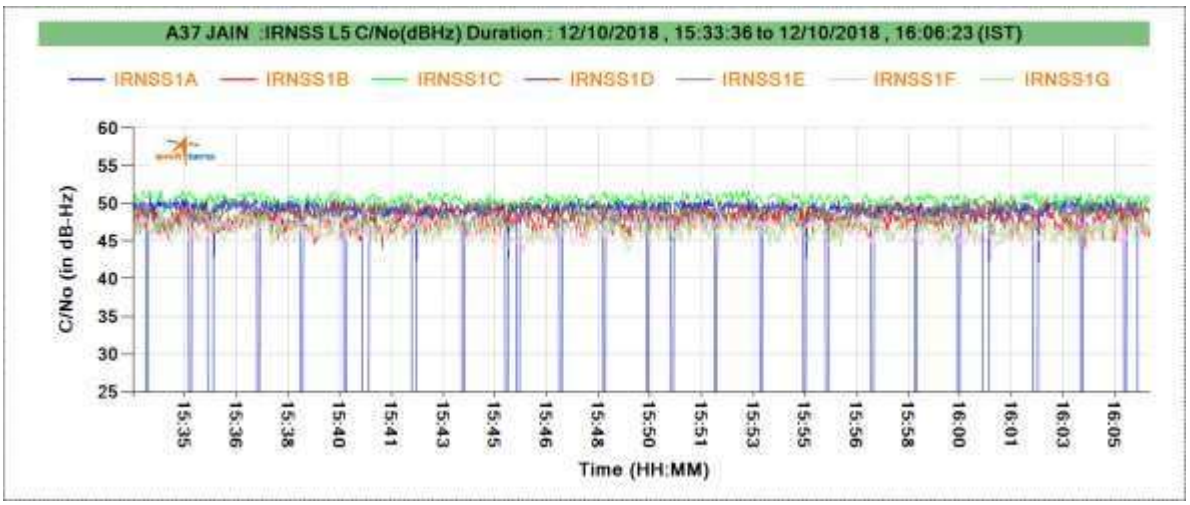

Fig .12(a) IRNSS L5 Band C/N_0

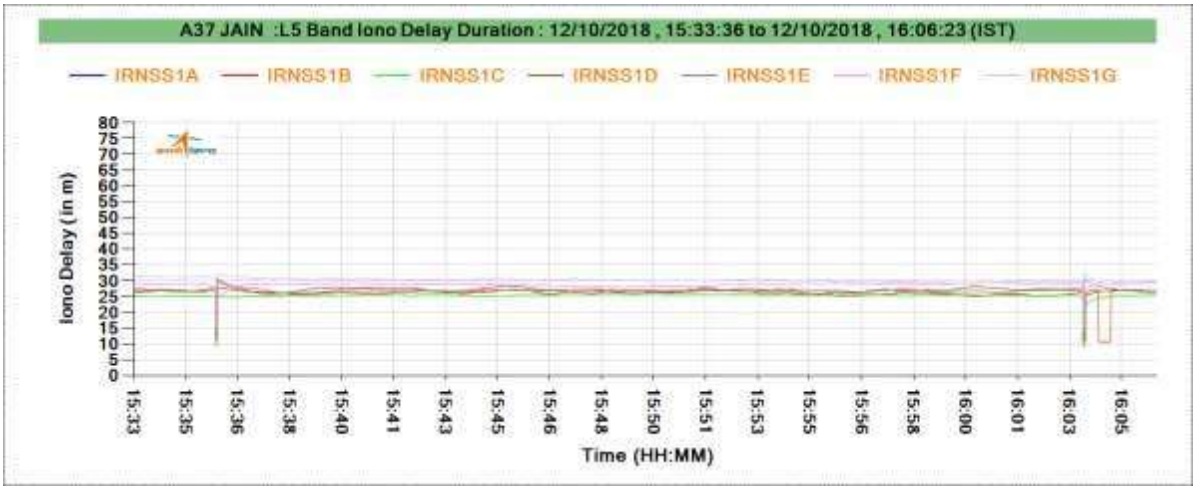

Fig .12(b) IRNSS L5 Band Iono Delay

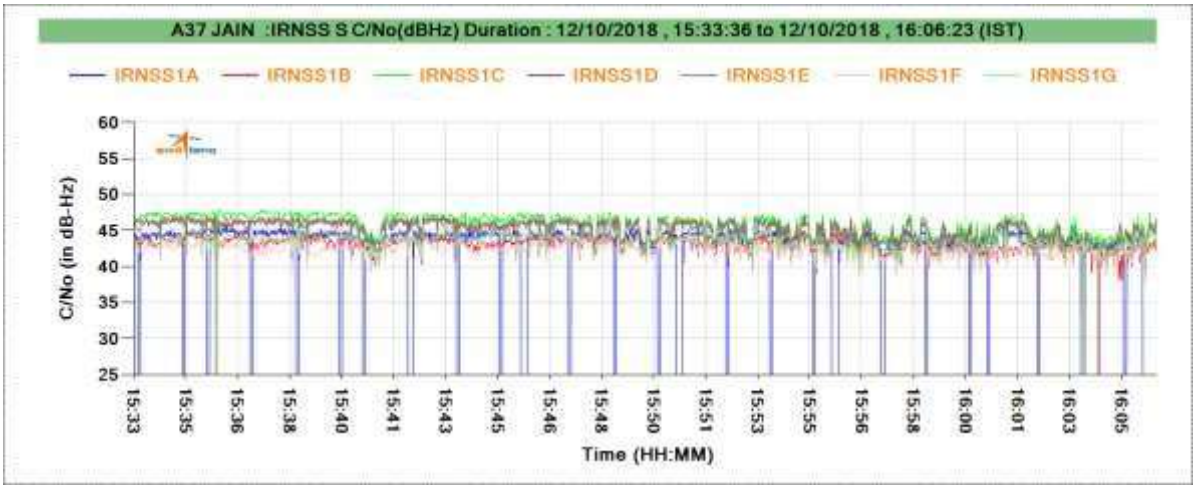

Fig .12(c) IRNSS S1 Band C/N_0

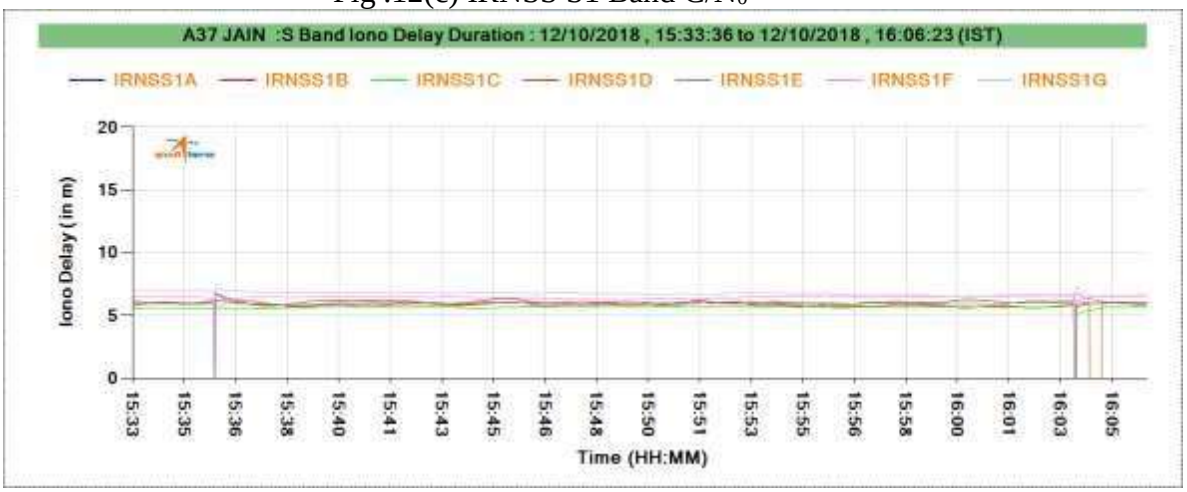

Fig .12(d) IRNSS S1 Band Iono Delay

IRNSS 1A to IG both L5 and S1 band and GPS L1 C/N0 and Iono delay observation plots shown in Fig. 12(a) to (d) based on the A38 in dynamic and A37 in static mode during the whole testing survey period. IRNSS C/N_0 varies from 48.37 to 50.9 whereas in case of GPS varies from 35.5 to 51.

Conclusion

When the signal travels in different layers of atmosphere it will be exposed to refraction and diffraction which makes the signal to degrade. The receiver is taken for the survey where the receiver is exposed to dense vegetation, Hills and building at different point of time. From this survey we can observe the multipath effect of the navigation signal in both static and dynamic modes. This depends on the distances between NavIC user receivers and by fixing these distances, the errors of each IRNSS/GPS receiver are found. The result of all the surveys shows that this method is applicable for real-time applications.

Acknowledgement

ISRO Grant No. NGP22 by utilizing this grant this research work was carried out. The authors like to acknowledge the support of Space Applications Centre - Indian Space Research Organization (SAC-ISRO) by providing IRNSS receiver and encouraging us to work on this navigation studies. Authors thank Dr. G. Raju & JAIN (Deemed-to-be University), Bangalore for the support to complete this work successfully. Scholar also acknowledges the Directorate of Minorities, Government of Karnataka for their Ph.D. Fellowship.

References

[1] Wang, G., K. de Jong, Q. Zhao, Z. Hu, and J. Guo (2015) "Multipath analysis of code measurements for BeiDou geostationary satellites," GPS Solutions, vol 19 no 1,
January, pp. 129–139. doi: 10.1007/s10291-014-0374-8

[2] Landau, H., M. Brandl, X. Chen, R. Drescher, M. Glocker, A. Nardo, M. Nitschke, D. Salazar, U. Weinbach, F. Zhang (2013) "Towards the inclusion of Galileo and BeiDou/compass satellites in trimble centerpoint RTX," in Proceedings of the ION GNSS 2013+, 16-20 September, Nashville, TN, pp. 1215–1223,

[3] Majithiya, P., K. Khatri K, and J. K. Hota (2011) "Indian regional navigation satellite system: correction parameters for timing group delays," Inside GNSS, vol 6, no 1,
January/February, Gibbons Media & Research LLC, Red Bank, NJ, pp. 40-46

[4] Mruthyunjaya, L. and A. S. Ganeshan (2014) Indian Regional Navigation Satellite System Standard Positioning Service Signal in Space Interface Control Document (IRNSS SPS SIS ICD), Version 1.0.

[5] Mohmad Umair Bagali, Dr. Thangadurai N, “Embedded System Interfacing with GNSS user Receiver for Transport Applications”, International Journal of Advanced Computer Science and Applications, Vol. 10, No. 9, pp.300-309, 2019.

[6] Mohmad Umair Bagali, Thangadurai N, “Application Specific Embedded Board Development Interfaced with GPS/IRNSS Receiver for Environmental Monitoring”, International Journal of Innovative Technology and Exploring Engineering, Vol.8, Iss.8, pp. 2628 – 2637,2019.

[7] W. Lechner and S. Baumann, "Global navigation satellite systems," Computers and Electronics in Agriculture, vol. 25, no. 1-2, p. 67–85, January

2000.
[8] A. Andrews, L. Weill, and M. Grewal, Global Positioning Systems, Inertial Navigation, and Integration, New Jersey: Wiley, 2007.
[9] M. Berber and N. Arslan, "Network RTK: A case study in Florida," Measurement, vol. 46, no. 8, pp. 2798-2806, October 2013.
[10] Sparkfun, "Description of Raspberry Pi - Model B," https://www.sparkfun.com/products/11546.
[11] "Satellite Navigation," Crosslink , p. 14, Summer 2002.
[12] R. Rizzi and A. Ortolani, Probabilistic Tomography of Atmospheric parameters from GNSS data, Bologna: University of Bologna, 2011.